

# Study of Wind Rate Measurement in a Venturi Tube System Equipped with two Water Filled Open Manometers

I Gede Rasagama

Lecturer, Department of Mechanical Engineering, Bandung State Polytechnic, Indonesia

**ABSTRACTS:** Various types of physical phenomena are experienced by the wind when it passes through a venturi tube system equipped with two open manometers filled with water. Its theoretical studies lead to 3 equation types of theoretical wind speeds that are unique. Experimental testing of each type of equation as a measurement method is significant to see the suitability level with the concept of fluid dynamics, the precision level, and the accuracy level. The research aims to determine the level of suitability with the fluid dynamics concept, the precision level, and the accuracy level. The research method is an experiment using equipment at the Bandung State Polytechnic Physics Laboratory. The research shows that: The suitability level of the three method measurement results is consistent with the concept of fluid dynamics; The highest level of precision and accuracy is produced by measurement method A, followed by method B, and the lowest by method C; All slopes of the linear curve mean wind speed ( $\bar{v}_a$ ) is negative, 83.3 % of absolute uncertainty (AU) < 0 (negative), and 83.3 % of relative uncertainty (RU) > 0 (positive); The determination level of  $v_a$  by the diameter variable (d) and the electrical resistance (R) is in a strong category, the determination level of AU by the variable d is in the moderate category but with the variable R is in the weak category and then the weak category for the determination level of RU by the variable d and with the variable R.

**KEYWORDS:** Wind Speed Measurement, Venturi Tube, Open Manometer, Measurement Precision, Measurement Accuracy

## 1. INTRODUCTION

### 1.1 Background

In industry, variable control of fluid (gas) flow rates plays an important role in producing quality processes and products. In the GTAW welding process, it has an impact on the hardness of low-carbon steel products [1]. In the natural gas well production process, its role is an indicator of the ability to deliver products to consumers [2]. In the corn-cob-biomass stove gasification process, its role is one of the determinants of the composition of gas-combustible products [3].

Fluid rate is one of the crucial concepts that is always analyzed in the topic of fluid dynamics. In fluid dynamics according to Clifford E. Swartz, analyzing this concept is among the most difficult applied sciences [4]. Contextualization in the Physics KBM, this concept is needed [5], one of which is the use of venturi tube and open manometer practicum equipment settings. On the other hand, understanding this phenomenon is also urgent for PT graduates such as chemical engineering, mechanical engineering, aeronautical engineering, and civil engineering as provisions when entering the industry [6, 7].

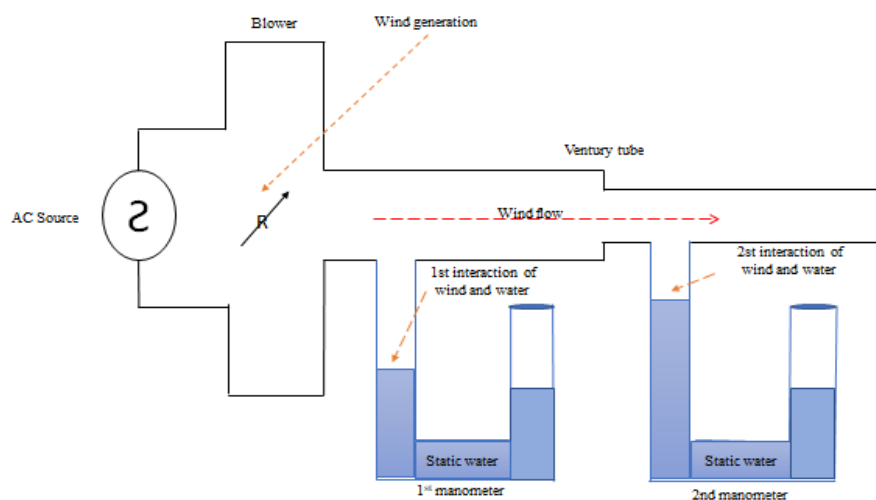


Fig. 1 Wind generation and interaction

A venturi tube is a flow constrictor along the fluid flow to produce a pressure difference [8, 9, 10, 11]. Manometers are fluid pressure gauges through the utilization of static fluid phenomena in U-pipes [12, 13]. These tools are critical to the industrial world. Venturi tubes are related to fluid rate control and manometers are related to fluid pressure control [14]. These two quantities are controlled for various purposes. Based on the application of these two tools, fuel and raw material efficiency, process effectiveness and safety, and production quality can be described.

The study of the physical phenomena of wind in a venturi tube and water in 2 open manometers as a system can be directed to obtain 3 methods of measuring the wind rate for the same position. Physical phenomenon 1 includes wind flowing from the source through the venturi tube, physical phenomenon 2 includes wind interacting with water in manometer 1, and physical phenomenon 3 includes wind interacting with water in manometer 2. The diameter of the venturi tube, the position of manometer 2 is different from that of manometer 1, as shown in Figure 1.

Wind generation in a venturi tube is a typical physical phenomenon, where the capacity of AC-sourced electrical energy in an electric motor is easily varied so that the kinetic energy and wind flow rate vary [15, 16]. The flexibility of the manometer position as a place or point of wind-water interaction gives rise to physical phenomenon 2 which is different from physical phenomenon 1. In this physical phenomenon, the wind rate varies even though the capacity of wind kinetic energy or electrical energy remains.

Comparison of physical phenomena of interaction points 1 and 2 is mathematically capable of inducing a new type of theoretical wind rate equation and is different from the type of theoretical wind rate equation based on physical phenomena 1 and 2, or 3. Base on controlling the function of the resistor in the blower system, the function of the venturi tube where the wind flows, and the 2nd function of the manometer where the water is located will lead to the generation of various types of typical physical phenomena. The study of experimentally verifying the theoretical wind speed equation based on physics symptoms 1, 2, or 3, and the results of the comparison of physical phenomena 2 and 3 is necessary to do to fulfill the need for knowledge regarding the verification of the concept of fluid dynamics, the effectiveness of measuring physical quantities in the laboratory, and other interests. other scientific interests.

**1.2 Theoretical Framework**

Physical phenomenon 1 in the form of magnetic force generation is one form of applying the energy conservation law with the electrical energy conversion into kinetic energy [17, 18]. Based on blower system technology, the rotational mechanical work of the electric motor is manipulated into wind kinetic energy in the venturi tube. If the wind density is expressed with  $\rho_a$ , the wind discharge is expressed with  $Q_a$ ,

and the wind rate is expressed with  $v_a$  means the kinetic energy per unit times or wind power generated by the blower system fulfills the equation:

$$P_a = \frac{1}{2} \rho_a Q_a v_a^2 \dots (1)$$

Manipulation of the venturi tube function through diameter variation, where  $v_a$  is observed,  $Q_a$  in equation (1) can be expressed as the product of the cross-sectional area of the venturi tube ( $A = \frac{1}{4} \pi d^2$ ) with  $v_a$ .  $P_a$  generated in physical phenomenon 1 is deformed into:

$$P_a = \frac{\pi}{8} \rho_a d^2 v_a^3 \dots (2)$$

Where  $d$  is the diameter of the venturi tube and the position of the wind and water interaction point. The source of wind generation energy per unit load is the AC PLN voltage. If the constant AC voltage is expressed as  $V_{PLN}$  and the variable electrical resistance is expressed as  $R$  and other electrical resistance is ignored, the amount of energy per unit time or electrical power for the operational purposes of the blower system fulfills the equation:

$$P_L = \frac{V_{PLN}^2}{R} \dots (3)$$

The existence of power losses in the conversion of electrical energy into wind energy causes wind power to be smaller than electrical power [19]. If the efficiency of the conversion symptom is expressed as  $\eta$ , the relationship between  $P_a$  and  $P_L$  results in the following equation  $v_a$ :

$$v_a = \sqrt[3]{\eta \frac{8V_{PLN}^2}{\pi \rho_a d^2 R}} \dots (4)$$

Equation (4) applies to physical phenomenon 1 at both interaction points 1 and 2 as the place of conversion of electrical energy into wind kinetic energy, with adjustment of type  $d$  between the two types of interaction points. Physical phenomena 2 and 3 are the different positions of the water surface on the arms 'a' of the manometer. This condition is the conversion result of wind kinetic energy into Earth's gravitational potential energy for water. When the water density is expressed as  $\rho_w$ , the Earth's gravitational acceleration is expressed as  $g$ , and the difference in the height of the water surface in each manometer is expressed as  $\Delta h_w$ , the relationship between the Earth's gravitational potential energy per unit volume received by water and the kinetic energy per unit volume given by the wind results in the equation  $v_a$  as follows:

$$v_a = \sqrt{\frac{2\rho_w g \Delta h_w}{\rho_a}} \dots (5)$$

Equation (5) applies to physical phenomena 2 and 3 at both interactions point 1 and 2 as the place of conversion of wind kinetic energy into gravitational potential energy of the water Earth, with adjustment of the type of difference in water surface height of the manometer arms between the two types of interaction points.

The movement of wind from physical phenomena 2 to 3 is a mass flow phenomenon due to work by because of a net force acting on the wind that is converted into wind kinetic energy.

“Study of Wind Rate Measurement in a Venturi Tube System Equipped with two Water Filled Open Manometers”

Assuming the wind is an incompressible, non-viscous fluid, and the flow is steady, then the motion of the wind from interaction points 1 to 2 satisfies the continuity equation and Bernoulli equation. If  $d$  interaction points 1 and 2, respectively expressed  $d_1$  and  $d_2$ ,  $\Delta h_w$  interaction points 1 and 2, respectively expressed  $\Delta h_{w1}$  and  $\Delta h_{w2}$  then  $v_a$  at interaction points 1 ( $v_{a1}$ ) and 2 ( $v_{a2}$ ) satisfy the equation:

$$v_{a1} = v_{a2} \left(\frac{d_2}{d_1}\right)^2 = \sqrt{\frac{2\rho_w g(\Delta h_{w1} - \Delta h_{w2})}{\rho_a \left(\left(\frac{d_1}{d_2}\right)^4 - 1\right)}} \dots (6)$$

Equations (4), (5), and (6) define three theoretical  $v_a$  equations, which apply to the same reference interaction points. Each equation contains several physical quantities that behave as constants, measurable, and in different formations.

**1.3 Problem Formulation**

Because of the study of the above physical phenomena, three theoretical  $v_a$  equations with different characteristics have been generated. Each  $v_a$  equation type is used as the theoretical basis for experimental  $v_a$  measurements. Supported by conditioning variations in the values of  $R$  and  $d$ , the  $v_a$  experimental study at each interaction point is more comprehensive and related to the scope of applicability of the concept of fluid dynamics. Each experimental  $v_a$  measurement through the application of the three theoretical  $v_a$  equation types will produce a certain suitability level to the fluid dynamics concept, precision, and accuracy and is unique.

The study aims to determine the quality of applied products of each type of theoretical  $v_a$  equation based on experimental measurement results in the Laboratory. Another study objective is to determine the best-applied product quality among the three theoretically  $v_a$  equation types after comparison. The quality of the applied products of the three

theoretical  $v_a$  equations is seen based on the level of suitability of the measurement results to the concept of fluid dynamics, the level of precision and accuracy of the experimental  $v_a$  measurement results, or the results of the application of each theoretical  $v_a$  equation in the Laboratory.

**2. METHODS**

**2.1 Tools**

The research utilized the Bandung State Polytechnic Physics Laboratory equipment, including one blower system equipped with a rheostat for setting nine different types of  $R$  (electrical resistance of the rheostat); 1 venturi tube equipped with eight interaction points with different  $d$ 's (diameter of the venturi tube wall), including points a, b, c, d, e, f, g, and h; 2 open manometers filled with pure water; 5 silicone connector hoses; 1 digital multimeter; 1 tube lamp for lighting; 1 caliper, and one ruler. The equipment design for the venturi tube and two open manometers is shown in Figure 2.

**2.2 Procedure**

Indirect measurement of experimental  $v_a$  involves three simultaneous physical phenomena. From 9 different types of  $R$  (1 type of  $R$  related to the measurement of 2 types of  $v_a$  coupled with different  $d$ 's), eight interaction points with different  $d$ 's, and three theoretical  $v_a$  equations for measurement (hereafter referred to as methods A, B, and C), this study produced 1512 different  $v_a$  and 135 different  $\bar{v}_a$ .

In 1 type  $R$ , 28 pairs of  $d$  were conditioned, including seven  $v_a$  points a paired with  $v_a$  points b, c, d, e, f, g, and h; 6  $v_a$  points b paired with  $v_a$  points c, d, e, f, g, and h; 5  $v_a$  points c paired with  $v_a$  points d, e, f, g, and h; 4  $v_a$  points d pair with  $v_a$  points e, f, g, and h; 3  $v_a$  points e pair with  $v_a$  points f, g, and h; 2  $v_a$  points f pair with  $v_a$  points g and h; and one  $v_a$  point g pairs with  $v_a$  point h

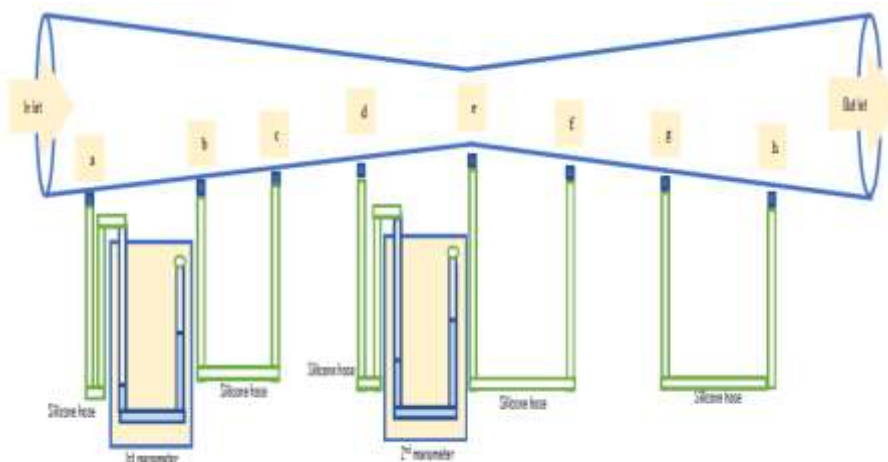


**Fig. 2. Major equipment design**

The specifications of the research physical quantities as the constants in equations (4), (5), and (6) are utilizing the results of previous research, as shown in Table 1.  $\Delta h_{w1}$  and  $\Delta h_{w2}$

were measured according to the conditions in the field.  $V_{PLN}$  as shown in Table 1,  $R$  and  $d$  inside the venturi tube,

respectively, were measured with the relevant equipment according to their specifications.

**Table 1. Specifications of research physics quantities**

N.	Types	Symbols	Value	SI units
1	Density of wind	$\rho_a$	1.22E+00	kg/m <sup>3</sup> [20]
2	Density of pure water	$\rho_w$	9.95E+02	kg/m <sup>3</sup> [21]
3	Earth's gravitational acceleration	g	9.80E+00	m/s <sup>2</sup> [22]
4	Blower system efficiency	$\eta$	5.33E-01	Unitless [23]
5	Voltage of PLN	V <sub>PLN</sub>	2.20E+02	Volt

**2.3 Data analysis**

Using an Excel application, all data was organized, differentiated, and processed based on categories A, B, and C based on the physical quantities that formed each theoretical  $v_a$  equation. Since each theoretical  $v_a$  equation is the theoretical basis of measurement, each category of data was processed by the corresponding method. From the application

of each method, the  $\bar{v}_a$ , AU, and RU of the measurement results of each method, the corresponding curve, slope, and coefficient of determination ( $R^2$ ) of the corresponding linear curve are known. This is the basis for analysis in determining the level of suitability with the concept of fluid dynamics, the level of precision, and the level of accuracy of each method. The flow of data analysis is shown in Figure 3.

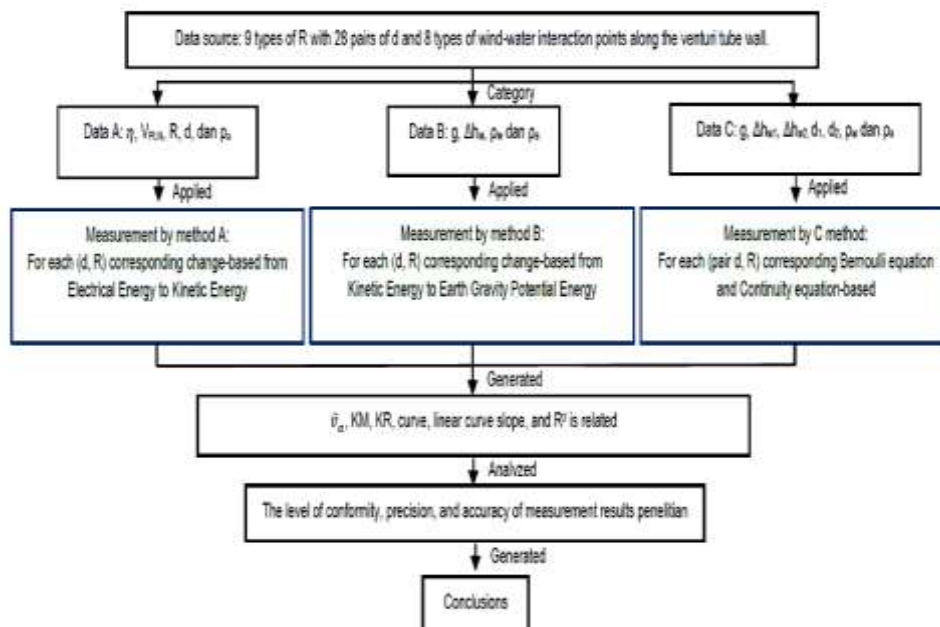


**Fig. 3. Data processing flow**

To analyze the level of suitability of the measurement results of each type of theoretical  $v_a$  equation with the concept of fluid dynamics, the tendency of the impact of the change of R when d remains and the change of d when R remains on  $\bar{v}_a$  is used both qualitatively and quantitatively. Qualitatively utilizing the tendency of the position and fluctuation of the  $\bar{v}_a$  curve of each method as  $f(d)$  when R remains and  $f(R)$  when d remains. Quantitatively utilizing the calculated results of  $\bar{v}_a$ , the slope of the curve or differentiation of  $\bar{v}_a$  when d changes but R remains, the slope of the curve or differentiation of  $\bar{v}_a$  when R changes but d remains,  $R^2$  for the correlation of  $\bar{v}_a$  with R when d remains, and  $R^2$  for the correlation of  $\bar{v}_a$  with d when R remains.

To analyze the level of precision of the  $v_a$  measurement results of each type of theoretical  $v_a$  equation, the tendency of the calculation results of AU of each method, the position and fluctuation of the AU curve of each method, the slope of the curve or differentiation of AU against d when R remains each method, the slope of the curve or differentiation against R when d remains each method,  $R^2$  on  $AU = f(d)$  when R remains each method, and  $R^2$  on  $AU = f(R)$  when d remains each method.

To analyze the level of accuracy of the  $v_a$  measurement results of each theoretical  $v_a$  equation, the tendency of the RU calculation results of each method, the position and fluctuation of the RU curve of each method, the slope of the curve or differentiation of RU against d when R remains each

method, the slope of the curve or differentiation against R when d remains each method, R<sup>2</sup> on RU = f (d) when R remains each method, and R<sup>2</sup> on RU = f (R) when d remains each method.

To determine the determination of the independent variable on the dependent variable, the linear regression method is used based on the slope of the curve and R<sup>2</sup>. In the linear regression method, the correlation of the dependent variable with the independent variable is linear [24]. The category of correlation level is strong if fulfill 67% < R<sup>2</sup> < 100%, moderate if fulfill 33% < R<sup>2</sup> < 67%, and weak if fulfill 19% < R<sup>2</sup> < 33% [25].

**3. FINDINGS AND DISCUSSION**

**3.1 Suitability level of experimental v<sub>a</sub> measurement results**

For R remains, the three experimental  $\bar{v}_a$  tend to get smaller as d gets greater, as shown in Figure 4. The correlation condition of the three methods is quantitatively verified by Table 2, where all the slopes of the curves  $\bar{v}_a = f(d)$ , R remains are negative with an average R<sup>2</sup> of 70% (strong category). It means that the three methods are characterized following the concept of the fluid dynamic, especially Bernoulli's law and the law of continuity. In every fluid dynamic phenomenon, the smaller the pipe d, the narrower the space for fluid movement, and the higher the compressive force by the pipe walls against the fluid. This condition increases the fluid's kinetic energy so that the rate of fluid motion is higher.

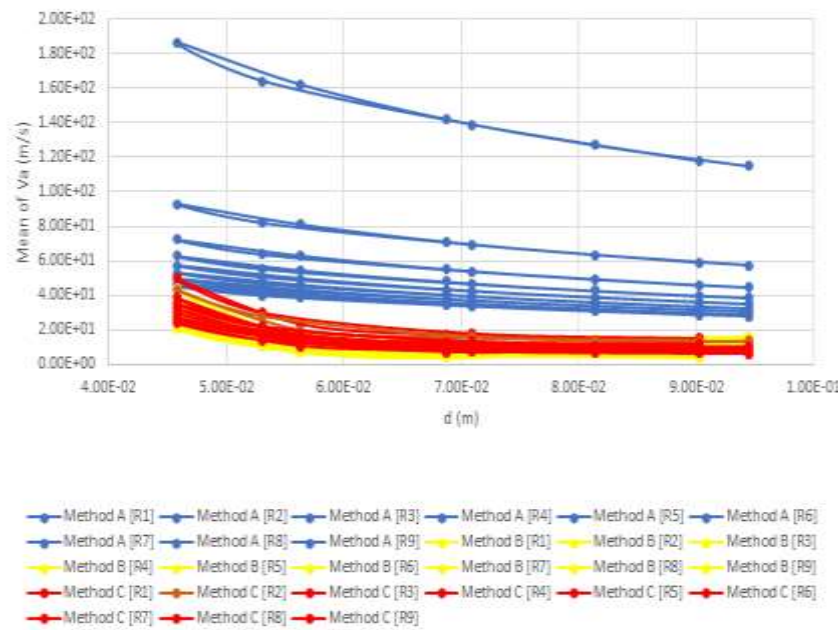


**Fig. 4.  $\bar{v}_a = f(d)$  on some R remains**

**Table 2. Curve slope and R<sup>2</sup> from  $\bar{v}_a$  experiment**

Method	d changes, R remains		R changes, d remains	
	Slope (ms <sup>-1</sup> /m)	R <sup>2</sup> (%)	Slope (ms <sup>-1</sup> /Ω)	R <sup>2</sup> (%)
A	-5.48E+02	97	-2.73E-01	58
B	-3.03E+02	46	-3.09E-02	79
C	-3.86E+02	67	-4.11E-02	92

Judging from the slopes of the curves of  $\bar{v}_a = f(d)$ , R remains in Figure 4 and Table 2, it appears that the largest negative slope belongs to the curve of  $\bar{v}_a = f(d)$  method A with the largest R<sup>2</sup>. The slopes of the other two curves appear to be smaller and thus gentler. Equation (4) shows that the dependence of v<sub>a</sub> on d is explicit, where the condition d<sup>2</sup> is inversely proportional to v<sub>a</sub><sup>3</sup>. The dependence of v<sub>a</sub> on d in equation (5) is implicit. Equation (6) shows the dependence of v<sub>a</sub> not on a single d but the ratio d of 2 interaction points along the venturi tube. The difference in the nature of the

dependence of the dependent variable on the independent variable is the cause of the difference in the slope of the curve  $\bar{v}_a = f(d)$  among methods A, B, and C.

Figure 4 also shows that the curve position of  $\bar{v}_a = f(d)$  from method A is mostly above that of methods B and C. This fact is supported by the fact that the overall  $\bar{v}_a$  values of the three methods are 5.73E+01 m/s for method A, 1.18E+01 m/s for method B, and 1.55E+01 m/s for method C, respectively. It means that the overall  $\bar{v}_a$  of method A is higher than that of the other two methods. The fluid flow rate equation from

method A base on the physical phenomenon in the system of 1 venturi tube and two manometers, whose existence is directly related to the energy source of the equipment system. The initial converted energy capacity is still quite large, then in the next stage of the physical phenomenon, the energy capacity decreases due to the impact of non-conservative forces. The difference in the result of  $\bar{v}_a$  among the three methods is closely related to the different assumptions of physical conditions as the basis of analysis in formulating the fluid flow rate equation.

For  $d$  remains, the  $\bar{v}_a$  of the three experimental method is smaller when  $R$  is larger, as shown in Figure 5. This fact is verified by Table 2 where the slope of the curve  $\bar{v}_a = f(R)$  of

the three methods is negative with a large  $R^2$  of 76% (strong category). The variable  $R$  affects the operational power of the wind generation system. As  $R$  increases, the operational power of the wind generation system decreases. On the other hand, the variable  $\bar{v}_a$  is an indicator of the quantity of wind mechanical energy, where a larger  $\bar{v}_a$  means a higher wind mechanical energy. There is a theoretical relationship where the variable  $R$  is inversely proportional to the variable  $v_a$ . Thus, the experimental facts of the three methods have demonstrated, supported, and matched the theoretical relationship between the variable  $R$  and the flow rate in the field of fluid dynamics.

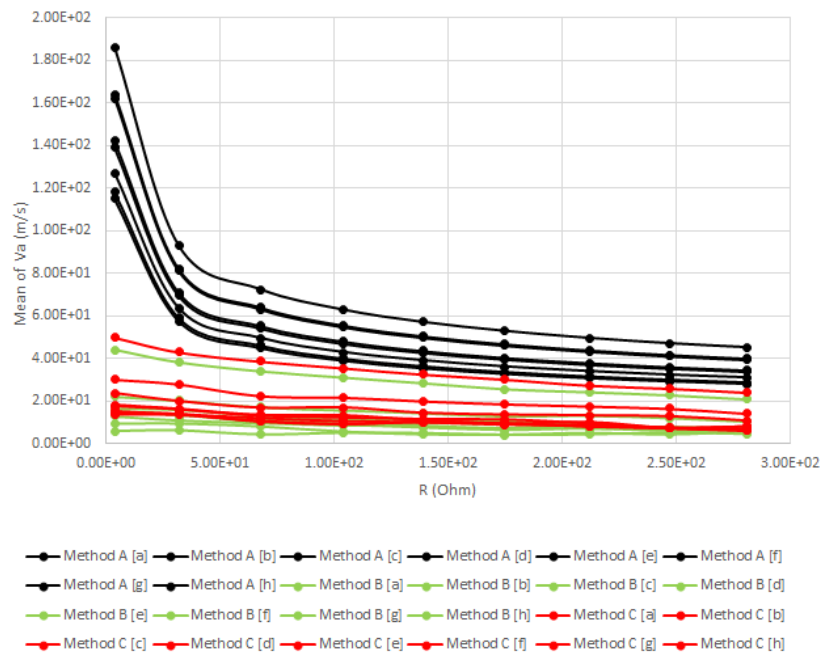


Fig. 5.  $\bar{v}_a = f(R)$  on some  $d$  remains

Regarding the slope of the curve  $\bar{v}_a = f(R)$ ,  $d$  remains, it appears that method A is sharper than methods B and C, as shown in Figure 5. This fact is verified by Table 2 where the slope of the curve is the largest with  $R^2$  above 50%. This experimental fact is like the phenomenon of the curve  $\bar{v}_a = f(d)$ ,  $R$  remains. The explicit relationship of  $v_a$  versus  $R$  exists only in equation (4) and not in the other two equations. The implicit relationship of  $v_a$  versus  $R$  in equations (5) and (6) is the reason why the slope of the curve  $v_a = f(R)$  in methods B and C is slower than the explicit relationship of  $v_a$  versus  $R$  in equation (4). The nature of the relationship between two variables in a physical equation or formula is an indicator of the level to which the slopes of the curves of the two types of variables are interrelated. Mathematically, the relationship between these two variables cannot be generalized, until there are detailed experimental tests in the laboratory.

The curve position of  $\bar{v}_a = f(R)$  of method A is mostly above that of methods B and C, as shown in Figure 5. This phenomenon is also like the  $\bar{v}_a = f(d)$  phenomenon ( $R$  remains) in Figure 4. It means that the experimental  $\bar{v}_a$  of

method A at each type of  $d$  and  $R$  studied is always higher than that of methods B and C. For the intervals of  $4 \Omega \leq R \leq 281 \Omega$  and  $4.58 \text{ mm} \leq d \leq 9.45 \text{ mm}$ , empirically the intervals of experimental  $\bar{v}_a$  values are  $2.79E+01 \text{ m/s} \leq \bar{v}_a \leq 1.86E+02 \text{ m/s}$  for method A,  $6.85E+00 \text{ m/s} \leq \bar{v}_a \leq 4.38E+01 \text{ m/s}$  for method B, and  $5.98E+00 \text{ m/s} \leq \bar{v}_a \leq 4.98E+01 \text{ m/s}$  for method C, respectively. Besides being caused by the nature of the relationship between the two related variables, another contributing factor is the difference in physical phenomena and assumptions of physical conditions as the theoretical basis for analyzing the formulation of each related theoretical fluid flow rate equation.

It was found that there is sophistication in the study of the suitability of this fluid dynamics concept. A theoretical relationship of 2 variables is implicit but through experimental studies, the relationship becomes explicit and conforms to the concept of fluid dynamics. Mathematically, equation (5) shows the variable  $v_a$  is independent of the variables  $d$  and  $R$ , while equation (6) shows the variable  $v_a$  is not a function of the variable  $R$ . However, experimental facts

“Study of Wind Rate Measurement in a Venturi Tube System Equipped with two Water Filled Open Manometers”

show the nature of the dependence of the variable  $v_a$  on either  $d$  and, or  $R$  is real. The theoretical facts are verified differently by the experimental facts.

**3.2 Precision level of experimental  $v_a$  measurement results**

The overall mean AU from the measurement results of methods A, B and C are  $6.29E-01$  m/s,  $7.19E-01$  m/s and

$5.64E+00$  m/s, respectively. This is consistent with Figures 6 and 7, where the tendency of the AU curve of method C is more volatile than that of methods A and B. The AU curve tendency of method B's is more fluctuating than method A.

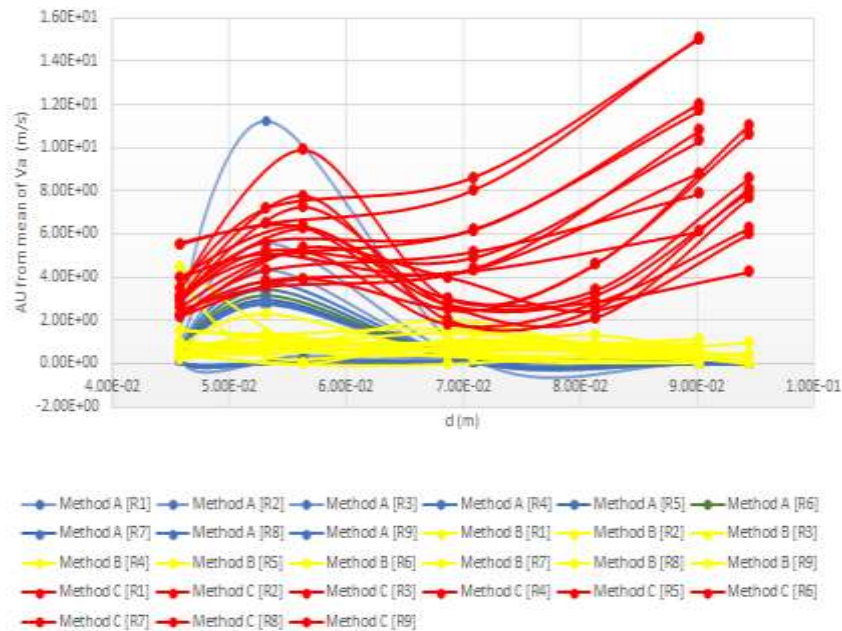


**Fig. 6. AU = f(d) on some R remains.**

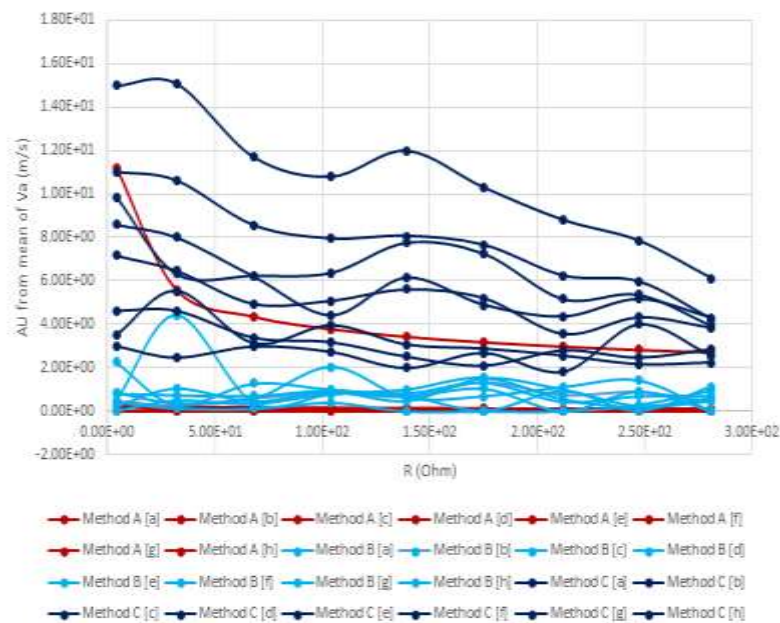


**Fig. 7. AU = f(R) on some d remains.**

The fluctuations of the AU curves in Figures 6 and 7 are verified by Table 3, where the slope of the AU curve for method C, both when  $d$  changes ( $R$  remains) and  $R$  changes ( $d$  remains) is largest at the highest  $R^2$ , compared to methods A and B. The slope of the AU curve of method B, both with

respect to  $d$  ( $R$  remains) and  $R$  ( $d$  remains) is the smallest compared to methods A and C. Under the conditions of  $AU = f(R)$  with  $d$  remains and  $AU = f(d)$  with  $R$  remains, the AU curve slopes majority for the measurement results by all three methods are negative. The average  $R^2$  of AU in these two

conditions is still  $< 45\%$ , not reaching the level of determination of  $\bar{v}_a = f(d)$  with R remains and  $\bar{v}_a = f(R)$  with d remains, where the average  $R^2$  is  $> 69\%$ .

**Table 3. Curve slope and  $R^2$  from AU experiment**

Method	d changes, R remains		R changes, d remains	
	Slope ( $\text{ms}^{-1}/\text{m}$ )	$R^2$ (%)	Slope ( $\text{ms}^{-1}/\Omega$ )	$R^2$ (%)
A	-3.67E+01	18	-3.00E-03	55
B	-1.34E+01	29	-8.50E-04	13
C	8.64E+01	30	-1.31E-02	63

The fact from the overall AU average, Figure 6, Figure 7, and Table 3 shows that the measurement results with the highest doubt occurred in method C, followed by methods B and A. The precision is the opposite of the hesitation of the measurement results. "Precision" refers to the level of measurement result reproducibility and measurement result consistency carried out repeatedly [26]. High precision means that the measurement results are very close to each other or give almost similar measurement results, or low measurement results variation, or deviation between 2 measurement results is very low. Thus, the category of precision level of methods A and B is higher than method C. The category of precision level of methods C among the other methods is the lowest. Regarding the condition of precision of methods A and B, it can be explained from the point of view of the practicality of the theoretical studies that underlie the equations of each measurement method. Historically, both these methods are based on the concept of energy conversion. Method B is still used and based on the ideal energy conversion concept, namely the law of conservation of mechanical energy, which ignores the effect of energy loss. Method A already considers the impact of inefficiency in the energy conversion phenomenon. It's the cause why the quality of precision of the measurement results of methods A and B is slightly different, where method A is more precise than method B both when d changes (R remains) and R changes (d remains).

The continuity equation and Bernoulli equation are the two fundamental equations, which is the basis of the measurement equation of method C. The continuity equation states that the dynamic fluid discharge (the volume flow rate) throughout the flow is the same, including when generated and flowed or when entering and exiting the pipe [27, 28, 29]. This statement does not correspond to reality (very difficult to realize) because the flow of leakage is difficult to avoid, especially since the phase of the dynamic fluid for research is gas. The research Bernoulli equation used is still idealized. It means that when applied, 100% of the drag effect is mechanical, and other factors in the real fluid are ignored [27, 28, 29]. The historical specificity of the equation for C method measurements does not appear to anticipate the

effects of repeated measurement. As a result, method C measurements for each type of variable produce the largest AU compared to methods A and B, so they have the lowest level of precision.

The differentiation of AU when d is getting bigger at R remains (Figure 6) and when R is getting bigger at d remains (Figure 7) shows similar tendencies as those shown in Figures 4 and 5, that is 83% negative slope. Based on the  $R^2$  comparison results in Tables 2 and 3, it is clear that  $R^2$  AU always  $< R^2 \bar{v}_a$ . The three methods for variable d (R remains) have a mean  $R^2 = 26\%$  for AU (Table 3) and a mean  $R^2 = 70\%$  for  $\bar{v}_a$  (Table 2). This category is weak. The three methods for variable R (d remains) had a mean  $R^2 = 44\%$  for AU (Table 3) and a mean  $R^2 = 76\%$  for  $\bar{v}_a$  (Table 2). This category is moderate. It indicates that the dependent variable AU is "less strongly differentiated or determined" than  $\bar{v}_a$  by the related independent variables. In the concept of physics, regarding the correlation of AU for  $v_a$  measurement results both when d changes (R remains) and R changes (d remains), especially in the field of fluid dynamic, "there is no concept" that describes both quantitatively and qualitatively. It is different for the correlation of fluid velocity with pipe diameter and the electrical resistance of mechanical energy generation systems with fluid velocity. On the other hand, the value of  $R^2$  must be interpreted as a high-low level of correlation between the dependent variable and the related independent variable. The smaller the  $R^2$  value, the lower the correlation between the two variables and vice versa. Thus, when the condition of d is larger (R remains) and when R is larger (d remains), the AU of the measurement results of the three methods tend to be smaller, but the correlation level is not the same as the correlation level of  $\bar{v}_a$  with the independent variable d (R remains) and the independent variable R (d remains).

**3.3 Accuracy level of experimental  $v_a$  measurement results**

Overall, the average RU of the experimental  $v_a$  measurement results of methods A, B, and C are 9.71E-01%, 8.02E+00%, and 4.63E+01%, respectively. This fact is confirmed by Figures 8 and 9 where the RU curve fluctuation of method C

“Study of Wind Rate Measurement in a Venturi Tube System Equipped with two Water Filled Open Manometers”

appears to be the highest, and the curve positions majority are above methods A and B. The fluctuation and position of the RU curve of method A is the opposite of method C.

Therefore, the largest RU is produced by method C measurements, followed by methods B and A.

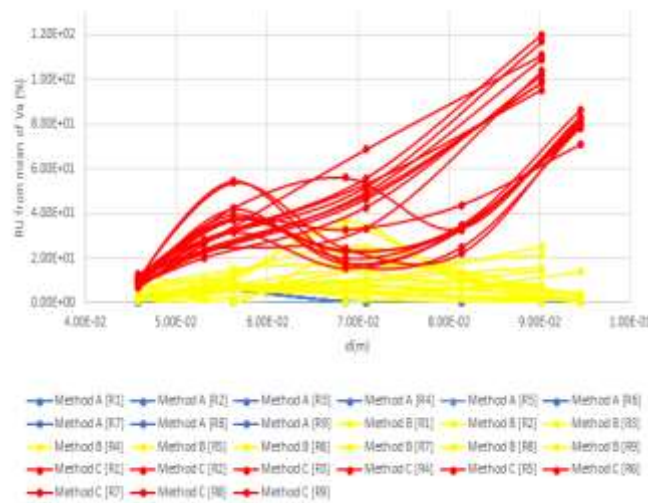


Fig. 8.  $RU = f(d)$  on some R remains.

Formulation for the study RU are used the ratio between the deviation by the measurement results mean [30]. Generally accepted or actual measurement results are the average of repeated measurement results. It is certain that the results of repeated measurements constantly fluctuate, or each measurement results with other measurement results must experience deviation. When the value of the measurement results is closer to the average measurement results, the deviation between the measurement results is smaller, as

consequently the RU of the measurement results is also smaller. On the other hand, the indicator of the accuracy of a measurement result is how far or close the value of the measurement results is to the generally accepted or actual measurement result or the average of repeated measurement results. Thus the accuracy category of method A is the highest compared to methods B and C. The accuracy category of method C is the lowest compared to methods A and B.

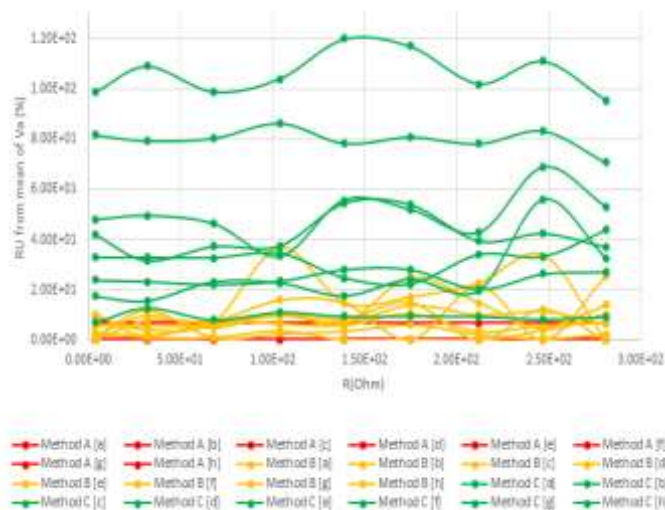


Fig. 9.  $RU = f(R)$  on some d remains.

This study utilized 1 type of equipment setting and several different physical phenomena in creating the three types of  $v_a$  equations. Data collection for each type of  $v_a$  equation was carried out during the measurement. Therefore, the differences in the accuracy of methods A, B, and C measurement results are certainly not related to differences in equipment types and conditions. Factors affecting the

accuracy conditions of the three methods are differences in the treatment of the physical phenomena underlying each  $v_a$  equation. These factors are like the factors affecting the precision of measurement results. The differences in treatment include: (1) differences in assumptions in utilizing physical phenomena during the formulation of the  $v_a$  equation; (2) differences in the stages of time of occurrence

regarding the physical phenomena selected to formulate the  $v_a$  equation so that resulting in a decrease in the capacity of converted energy from stage 1 physical phenomena to the

next stage; and (3) the application of different physical concepts among the physical phenomena selected to formulate the  $v_a$  equation.

**Table 4. Curve slope and  $R^2$  from RU experiment**

Method	d changes, R remains		R changes, d remains	
	Slope ( $m^{-1}$ )	$R^2$ (%)	Slope ( $\Omega^{-1}$ )	$R^2$ (%)
A	-5.58E+01	18	7.66E-18	11
B	2.68E+01	12	1.60E-02	14
C	1.47E+03	65	1.65E-01	35

The RU differentiation of the experimentally measured  $v_a$ , both due to the variable d (R remains) and R (d remains) appear to show different tendencies compared to the differentiation of  $\bar{v}_a$  and AU. Table 4 shows that the majority tendency of the RU slopes of the three methods is positive. However, this tendency with  $R^2$  is not the same as  $R^2$  of differentiation  $\bar{v}_a$  and AU, where the average  $R^2$  is 31% for correlation of RU with d for R remains (weak category), and 20% for correlation of RU with R for d remains (weak category). This fact justifies the proportionality correlation or comparability correlation, both when d gets bigger (R remains) and R gets bigger (d remains), where resulting in RU getting bigger.

**CONCLUSIONS**

The three theoretical  $v_a$  equations can produce measurements following the concept of fluid dynamics with the slope of the  $\bar{v}_a$  curve being negative and the determination level of  $\bar{v}_a$  by the two independent variables of the study categorized strongly. When d changes (R remains), the measurement of method A produces the highest differentiation of  $\bar{v}_a$  with a strong determination level, followed by method C with a strong determination level and method B with a moderate determination level. When R changes (d remains), method A's measurement yields the highest  $\bar{v}_a$  differentiation with the moderate determination level, followed by method C at the strong determination level and method B at the strong determination level. In the d and R intervals of the study, method A measurements yielded the highest overall  $\bar{v}_a$ , followed by methods C and B. The highest level of precision was produced by measurements of method A, followed by methods B and C. AU tends to be influenced by the two independent variables of the study on the curve slope being negative. The category of the AU determination level by the independent variable d is weak, and the variable R is moderate. The highest level of measurement accuracy was produced by measurement of method A, followed by methods B and C. RU tends to be influenced by the two independent variables of the study in the positive curve slope. The category of RU determination level by both independent variables d and R is weak. Thus, the type of method that

produces the first best measurement quality is method A, the second best is method B and the third best is method C.

**REFERENCES**

1. Dwiyati, S. T., Susetyo, F. B., & Yudhantono, A. D. P. (2018). Pengaruh Laju Aliran Gas Terhadap Nilai Kekerasan Baja Karbon Rendah Hasil Hardfacing Dengan Proses GTAW. *Jurnal Konversi Energi dan Manufaktur UNJ*, 5(1), 1-6.
2. Taufik, M. (2009). *Pemodelan Matematis Untuk Menghitung Kemampuan Produksi Sumur Gas. Bandung: Universitas Padjajaran–Fisika FMIPA.*
3. Wibowo, W. A., & Afriyadi, H. M. (2014). Pengaruh laju alir udara dan tipe aliran udara terhadap kinerja kompor gasifikasi tongkol jagung. *Ekulibrium*, 13(1), 7-10.
4. Swartz, C. E. (1981). *Phenomenal physics.* John Wiley & Sons.
5. Lilia, L., & Widodo, A. T. (2014). Implementasi pembelajaran kontekstual dengan strategi percobaan sederhana berbasis alam lingkungan siswa kelas X. *Jurnal Inovasi Pendidikan Kimia*, 8(2).
6. Deen, W. M. (2016). *Introduction to Chemical Engineering Fluid Mechanics.* Cambridge University Press.
7. Escudier, M. (2017). *Introduction to engineering fluid mechanics.* Oxford University Press.
8. Rofik, D. A. (2020). PERANCANGAN DAN ANALISIS ALAT MICROBUBBLE GENERATOR (MBG) UNTUK AERASI KOLAM IKAN TIPE NOZZEL VENTURI. *Gorontalo Journal of Infrastructure and Science Engineering*, 3(2), 24-30.
9. Hakim, L. (2004). Perancangan dan Pembuatan Alat Uji Karakteristik Pompa Sentrifugal Susunan Seri dan Paralel.
10. Tentua, B. G. (2015). Penerapan Helmholtz Resonator dan Air Blower Pada Karburator Skep Venturi Untuk Mengurangi Emisi Gas Buang Motor Honda. *Arika*, 9(2), 135-142.

11. Ismail, N. R. (2010). Optimalisasi Waktu Pada Saat Akselerasi Mesin Toyota 4 AFE dengan Memanipulasi Manifold Absolute Pressure (MAP). *Agritek*, 11(1), 1-8.
12. Solihat, I. (2019). SIMULASI PEGUKURAN TEKANAN UDARA MENGGUNAKAN MANOMETER SEDERHANA. *Jurnal Inovasi Ilmu Pengetahuan dan teknologi*, 1(1), 16-20.
13. Siregar, J. F., & Sinaga, J. B. (2013). Perancangan alat uji gesekan aliran di dalam saluran. *Jurnal Ilmiah Teknik Mesin*, 1(1).
14. Siregar, J. F., & Sinaga, J. B. (2013). Perancangan alat uji gesekan aliran di dalam saluran. *Jurnal Ilmiah Teknik Mesin*, 1(1).
15. Siregar, L., & Sibarani, A. N. (2020). Studi Analisis Perubahan Putaran Motor Induksi 1 Fasa Akibat Output PLTS Aplikasi Kipas Angin. *Jurnal ELPOTECs*, 3(2), 7-14.
16. Yulizar, A., Zondra, E., & Monice, M. (2021). Studi Konsumsi Energi Terhadap Perubahan Kecepatan dan Beban Pada Motor Induksi Tiga Fasa. *SainETIn: Jurnal Sains, Energi, Teknologi, dan Industri*, 6(1), 23-31.
17. Issetyorini, A., & Antono, D. (2012). Gaya Gerak Listrik Pada Motor AC. Jurusan Teknik Elektro. Politeknik Negeri Semarang.
18. Ulum<sup>1</sup>, M., Anshory, I., Saputra, D. H. R., & Ayuni, S. D. (2021). Arduino Based Multifunction Fan Kipas Angin Multifungsi Berbasis Arduino. *Procedia of Engineering and Life Science Vol*, 1(2).
19. Yolnasdi, Y., Ermawati, E., & Halim, A. (2022). ANALISA EFISIENSI MOTOR KAPASITOR SEBAGAI PENGGERAK ALAT UJI RUGI-RUGI ALIRAN FLUIDA. *JURNAL SAINSTEK*, 5(1).
20. Maulana, Y., & Astuti, K. Y. (2019). STUDI EKSPERIMEN TURBIN ANGIN BERSUMBU VERTIKAL UNTUK PJU (PENERANGAN JALAN UMUM). *Prosiding Hasil-Hasil Penelitian Tahun 2019 Dosen-Dosen Universitas Islam Kalimantan*.
21. Gideon, S., & Tarigan, E. (2020). Penentuan Massa Jenis Oli secara Sederhana dengan Hukum Archimedes. *Physics Education Research Journal*, 2(1), 43-50. doi:<https://doi.org/10.21580/perj.2020.2.1.5058>
22. Suratmi, S., & Zakiya, H. (2017). Perbandingan Ketelitian Nilai Percepatan Gravitasi Bumi Dengan Eksperimen Gerak Jatuh Bebas Dan Getaran Zat Cair di Politeknik Negeri Bandung.
23. Ahmad, A., Zondra, E., & Yuvendius, H. (2020). Analisis Efisiensi Motor Induksi Tiga Fasa Akibat Perubahan Tegangan. *SainETIn: Jurnal Sains, Energi, Teknologi, dan Industri*, 5(1), 35-43.
24. Ghozali, I. (2016). Aplikasi Analisis multivariete dengan program IBM SPSS 23 (Edisi 8). Cetakan ke VIII. Semarang: Badan Penerbit Universitas Diponegoro, 96.
25. W. W. Chin, (1998). “The partial least squares approach to structural equation modeling. Modern methods for business research”, Volume 295 Nomor 2, pp 295-336, Tahun 1998
26. Chan, C. C., Lam, H., Lee, Y. C., & Zhang, X. M. (Eds.). (2004). Analytical method validation and instrument performance verification (Vol. 18). ^ eNew Jersey New Jersey: John Wiley & Sons.
27. D. Halliday, R. Resnick, & J. Walker, *Fundamentals of Physics, Extended*, 11th Edition. New York: John Wiley & Sons. 2018
28. Giancoli, Douglas C., *Physics: Principles with Applications*, Seventh Edition, Boston: Pearson, 2016.
29. H.D. Young and R.A. Freedman. *University Physics with Modern Physics*. 14th Global Edition. Boston: Pearson Education Limited. 2016.
30. Gao, Y., Ierapetritou, M. G., & Muzzio, F. J. (2013). Determination of the confidence interval of the relative standard deviation using convolution. *Journal of Pharmaceutical Innovation*, 8, 72-82.